Generation and Assessment of VMF1-Type Grids Using North-American Numerical Weather Models

Landon Urquhart, Marcelo C. Santos, Felipe G. Nievinski, and Johannes Böhm

Abstract

Numerical weather models (NWM) have become an important source of atmospheric data for modeling error sources in geodetic positioning. One example of this is the development of the Vienna Mapping Functions (VMF1) and ray-traced zenith delays which are derived from the European Centre for Medium-range Weather Forecasts (ECMWF) datasets. These products are provided on an operational basis through the GGOS Atmosphere project. In general, relatively little consideration has been given to the choice of NWM on the derived mapping functions and zenith delay products. In this investigation we compare the gridded-VMF1 mapping functions and ray-traced zenith delays derived from the ECMWF to equivalent products derived by ray-tracing through the National Center for Environmental Prediction (NCEP) Reanalysis model. We have chosen to compare the gridded version of these products as they are available for any location on Earth, rather than only specific stations and have been shown to be essentially equivalent in terms of accuracy. This paper also includes a discussion about a systematic production of gridded-VMF1 and ray-traced zenith delays derived from the NCEP datasets (and from the Canadian Meteorological Center GEM model) on an operational basis. The benefits of the service would include: (1) a backup in the event of the ECMWF VMF1 or zenith delays being unavailable; (2) greater compatibility with other NWM derived corrections, such as atmospheric pressure loading and; (3) the availability of tropospheric delay products derived from an independent source and ray-tracing algorithms should provide more robustness for combination products which use these models.

Keywords

Mapping functions • Neutral atmosphere • Tropospheric delay • Vienna Mapping Functions

1 Introduction

In recent years, numerical weather models have been used operationally to improve the accuracy of space geodetic techniques. The Vienna Mapping Function 1 (VMF1) Service, which falls under the Global Geodetic Observation System: Atmosphere (GGOS Atmosphere http://ggosatm.hg.tuwien.ac.at/), provides ray-traced zenith delays and slant factor models derived from numerical weather model data on a 6-h basis, which can then be applied

L. Urquhart • M.C. Santos (✉)
Department of Geodesy and Geomatics Engineering, University of New Brunswick, P.O. Box 4400, Fredericton, NB, Canada E3B 5A3
e-mail: msantos@unb.ca

F.G. Nievinski
Department of Aerospace Engineering Sciences, University of Colorado, Boulder, CO, USA

J. Böhm
Institute of Geodesy and Geophysics, Vienna University of Technology, Vienna, Austria

C. Rizos and P. Willis (eds.), *Earth on the Edge: Science for a Sustainable Planet*, International Association of Geodesy Symposia 139, DOI 10.1007/978-3-642-37222-3_1,

for modeling the tropospheric delays in space geodetic observations.

The VMF1 mapping functions have been shown to be the most accurate mapping function to date (Tesmer et al. 2007). They are currently recommended for all precise geophysical applications, in particular if geophysical signals are to be investigated (Boehm and van Dam 2009). At this time the processing centers contributing to the International GNSS Service (IGS) have not adopted the VMF1 in the operational analysis routines, which may be due to concerns in the products availability. The VMF1 mapping functions are recommended by the International Earth Rotation and Reference Systems Service (IERS) in their most recent publication of the IERS Conventions (Petit and Luzum 2010).

The provision of a UNB VMF1-like service would improve the availability of VMF1 mapping functions making it less likely of a disruption in the service. Additionally, the independent source of the VMF1 mapping functions and the ray-traced zenith delays may be beneficial in improving the robustness of the IGS/IERS combined products as it would provide an independent source for tropospheric corrections. A UNB service would also act as a basis for developing improved tropospheric products such as azimuth-dependent VMF1 or ray-traced slant factors at the observation level.

First, a review of the current VMF1 service is provided. Next, we describe the benefits to providing an alternative source of corrections to the geodetic community. Finally, we look into the implementation of the VMF1-like service, discussing the distribution to users, NWM data provider and ray-tracing algorithms.

2 VMF1 Service

This is the current state-of-the-art approach to modelling the troposphere delay as recommended by the latest IERS Conventions (Petit and Luzum 2010):

$$\Delta L = \Delta L_{\mathrm{h}}^{z} \cdot mf_{\mathrm{h}}(e) + \Delta L_{\mathrm{w}}^{z} \cdot mf_{\mathrm{w}}(e) + mf_{\mathrm{G}}(e) \cdot [G_{\mathrm{N}} \cdot \cos(\alpha) + G_{\mathrm{E}} \cdot \sin(\alpha)] \tag{1}$$

where ΔL is the total delay, the two ΔL^{z} represent the zenith delay for the hydrostatic ("dry") and non-hydrostatic ("wet") components (indicated by subscripts *h* and *w*, respectively), *mf* (*e*) is the mapping function, as a function of the elevation angle *e* for the hydrostatic (subscript *h*), wet (subscript *w*) and for the gradient (subscript *G*). The two troposphere gradient parameters are represented by G_{N} and G_{E}, and α indicates the azimuth. The mapping function *mf* is the concern of this paper, and can be determined by the Vienna Mapping Functions 1.

Table 1 Coefficients for the VMF1 mapping function

Hemisphere	c_0	c_{10}	c_{11}	ψ
Northern	0.062	0.001	0.005	0
Southern	0.062	0.002	0.007	π

The VMF1 service relies on a numerical weather model produced by European Centre for Medium-range Weather Forecasts (ECMWF) and is implemented on the super-computing facilities of the ECMWF. The underlying functional formulation for describing the elevation angle dependence of the tropospheric delay is given by Marini (1972), normalized to yield unity at the zenith by Herring (1992):

$$mf(e) = \frac{1 + \frac{a}{1 + \frac{b}{1+c}}}{\sin e + \frac{a}{\sin e + \frac{b}{\sin e + c}}} \tag{2}$$

In a preliminary fit, all a_{h}, b_{h}, and c_{h} coefficients for the hydrostatic mapping function are determined from a least-squares fit of ray-traced observations taken at nine elevation angles, through monthly mean profiles of the ECMWF 40-year reanalysis data to Eq. (1). Then the b_{h} coefficient is held fixed to its mean value, equal to 0.0029, while the c_{h} coefficient is re-fit to the expression:

$$c = c_0 + \left[\left(\cos\left(\frac{doy - 28}{365.25} 2\pi + \psi\right) + 1\right) \frac{c_{11}}{2} + c_{10}\right] \times (1 - \cos\phi) \tag{3}$$

where *doy* is the day-of-the-year, ψ specifies either the northern or southern hemisphere (values 0 and π, respectively), and φ is the station latitude. Bear in mind that the values of the coefficients as shown in Table 1 in (Boehm et al. 2006b) are not correct.

The b_{w} and c_{w} coefficients for the non-hydrostatic mapping function were deemed to be less important as the non-hydrostatic delay is typically ten times smaller than the hydrostatic and therefore the coefficients remain to be fixed to those of the NMF (Niell 1996) at the 45° elevation angle, where b_{w} and c_{w} equal 0.00146 and 0.04391 respectively.

The final *a* coefficient is determined by ray-tracing through the ECMWF analysis on a 6-h basis at an initial elevation angle of 3.3° and then inverting Eq. (2) with *b* and *c* fixed as above. In this case, the corresponding outgoing elevation angle, which should be equal to approximately 3°, must be determined from the ray-tracing procedure in order to solve for the *a* coefficient. This approach is used for both the hydrostatic and non-hydrostatic mapping functions.

Originally, the VMF1 was produced on a site-specific basis. However, this was seen as a limitation as it constrained its use to only those stations for which the coefficients were computed. For this reason, the VMF1-grid coefficients are produced to allow users to simply interpolate the coefficients to the required location. Kouba (2008) showed that the difference between the gridded and site VMF1 are negligible and therefore the VMF1-grid is more desirable as it can be applied for all locations.

In the case of the VMF1-grid, the *a* coefficients are provided on a $2.0° \times 2.5°$ latitude/longitude grid. They are computed every 6 h at 0, 6, 12, and 18 UTC at ellipsoidal heights corresponding to the grid nodes of a global topography model (file *orography_ell*). The *a* coefficients are then reduced to the ellipsoid and these "zero height" values are the ones provided to end-users; in order to apply them, the subroutine *vmf1_ht.m* (which is available at: http://ggosatm.hg.tuwien.ac.at/DELAY/SOURCE/) must be used which applies a height correction to determine the *a* coefficient for the actual station height. The height correction to obtain the coefficient at the actual station height during grid usage is simply the inverse of the height reduction to obtain the coefficients on the ellipsoid during grid generation.

In addition to the mapping function, the zenith hydrostatic and non-hydrostatic delays are also provided in the gridded format. The zenith delays are provided at mean grid heights corresponding to the ellipsoid height in *orography_ell* and the zenith delays must be corrected for the difference in the gridded height and the actual station height. Several options are available and they are discussed in Kouba (2008) and Fund et al. (2009). This correction is performed by the user and is not part of the VMF1-service.

3 The UNB VMF1 Implementation

The geodetic community is now in a transition from corrections based on relatively simple closed-form mathematical models to corrections based on large amounts of external data. The VMF1 service is only one example of this shift. Even though the VMF1 mapping functions have been shown to be an improvement over the Global Mapping Functions (Boehm et al. 2006a) and Niell Mapping Functions (Niell 1996), at this time they have not been widely adopted for operational use even though they are currently recommended by the IERS Conventions (Petit and Luzum 2010). An alternative service provider could improve the availability of the products should the original VMF service become unavailable and perhaps make the use of the VMF1 corrections more appealing.

An alternative source of mapping functions and ray-traced zenith delays could improve the robustness of the IGS/IERS combined solutions as it would provide an independent source of corrections which could be applied by the analysis centers. When producing the IGS combined products the results from all analysis centers are combined in a least squares approach, even though in reality many of these solutions are highly correlated due to applying the same correction models and some analysis centers even using the same software. A UNB VMF1-like service would provide slant factor models based on an independent weather model and ray-tracing algorithms which would make the IGS combined solution more robust if the IGS did choose to switch to the VMF1 for operational use.

As was shown in Urquhart (2010) there exists a small latitude dependent bias in the VMF1 hydrostatic mapping function which is believed to be due to the assumption of a sphere of constant radius of the earth in the ray-tracing algorithms. This systematic bias results in an approximately 2 mm change in station height at the poles and at the equator. Although small, this systematic bias may be important for geophysical studies and for establishing reference frames. This will be further discussed below.

The UNB VMF1-like implementation is based on NOAA-NCEP reanalysis for operational purposes, but can also utilize the CMC-GEM models for comparison and quality control. In this investigation Numerical weather data available at every 6 h is used and the gridded version of the VMF1/UNB-VMF1 is compared which uses a $2.0° \times 2.5°$ latitude/longitude grid. The same empirical expressions for the coefficients *b* and *c* were employed to maintain consistency with the original VMF1. The impact of this assumption on accuracy will be assessed in the future. Validation data was provided by using independent three dimensional ray-traced observations. The ray-tracing algorithms used in the UNB implementation of the VMF1 are those described in Nievinski (2009).

4 Assessment

Several tests were made in order to evaluate the UNB implementation of the VMF1. The data set considered covers the whole of 2010, at four epochs daily (every 6 h), unless otherwise stated.

4.1 Zenith Delay Comparisons

The first comparison involves zenith delays derived from the ECMWF and NCEP weather models. Figure 1 shows the zenith hydrostatic delay difference between a the VMF1 solution based on the ECMWF and the UNB solution based on NCEP re-analysis. There are several outliers present which cause the extended colour bar in both cases. At this time it was not determined which product was the

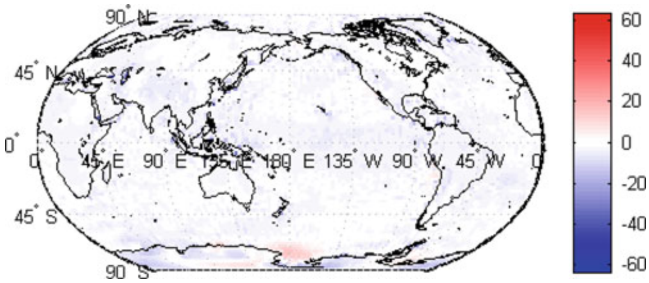

Fig. 1 Hydrostatic zenith delays (ECMWF − NCEP); *colour bar* in mm for the full year of 2010, four epochs daily

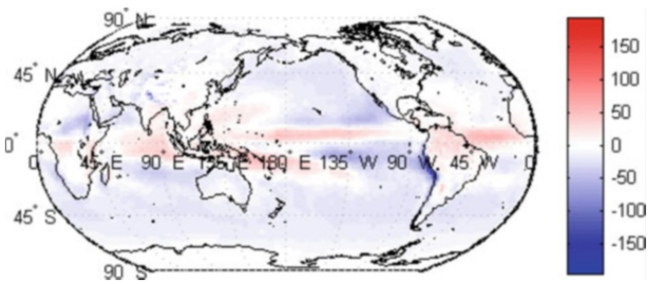

Fig. 2 Non-hydrostatic zenith delays (ECMWF − NCEP); *colour bar* in mm for the full year of 2010, four epochs daily

source of these outliers. For the hydrostatic delays there are several larger values occurring in Europe (and some also in Antarctica), while for the non-hydrostatic delay (shown in Fig. 2) the larger differences occur along the western coast of South America. There are some interesting effects in the equatorial region for the non-hydrostatic delays; most differences, though small, are over the oceans. Statistics for the hydrostatic delay are -2.4 ± 3.8 mm, whereas that for the non-hydrostatic delay it was found to be -6.3 ± 14.7 mm.

4.2 Comparison with Saastamoinen

A comparison using Saastamoinen (1972) zenith hydrostatic delay as truth is shown in Fig. 3, for 60 days (January and February, 2010). Input meteorological values were obtained from the station met files provided on the CDDIS data server. There is good agreement in the mean, but the UNB (NCEP) zenith hydrostatic delays tend to be noisier than the ECMWF zenith hydrostatic delays. This is believed to be due to the interpolation of the NCEP pressure levels fed to the UNB ray-tracer. Statistics contained in Table 2 are just for the stations shown in Fig. 3.

An analysis adding CMC zenith delays into the comparison was made for a 2-week period in 2008. In Fig. 4 we see the comparison of the zenith hydrostatic delay with respect to Saastamoinen. Notice that both the CMC and

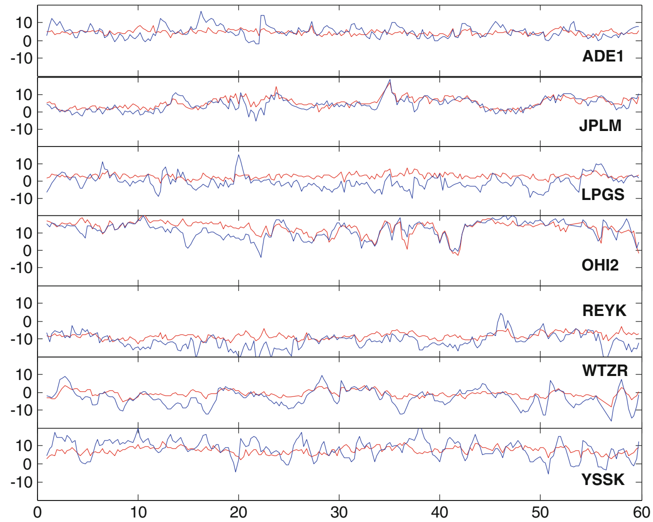

Fig. 3 Comparison with respect to Saastamoinen delays: *red* is for ECMWF (Vienna); *blue* is for NCEP (UNB). *Horizontal axis* indicates days, *vertical* is discrepancy in mm

Table 2 Average statistics over stations

Zenith hydrostatic delay	Bias	Standard deviation
ECMWF (Vienna)	3.3 mm	2.2 mm
NCEP (UNB)	2.0 mm	4.2 mm

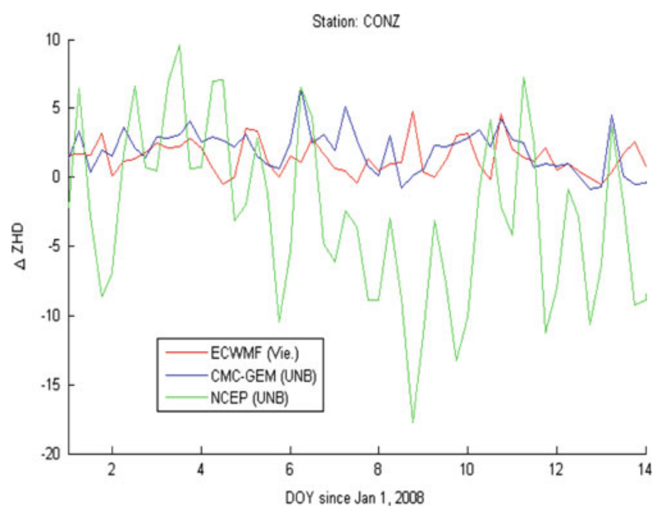

Fig. 4 Comparison with respect to Saastamoinen delays: *red* is for ECMWF (Vienna); *blue* is for CMC-GEM (UNB); and *green* for NCEP (UNB). *Horizontal axis* indicates days, *vertical* is discrepancy in mm

ECMWF results agree very well, both in bias and standard deviation with respect to the met-driven Saastamoinen. This was expected as we have performed significant more tests on the use of CMC in ray-tracing. Further work is required to identify the cause of the noisier results using NCEP.

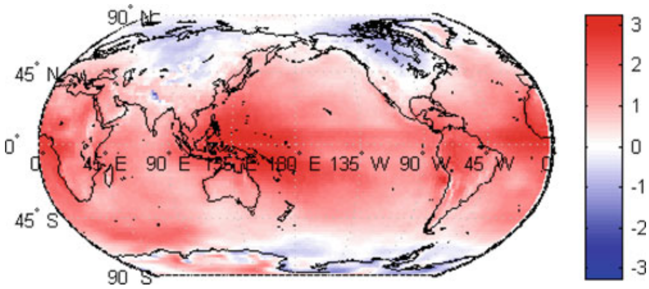

Fig. 5 Hydrostatic station height difference (ECMWF − NCEP); *colour bar* in mm

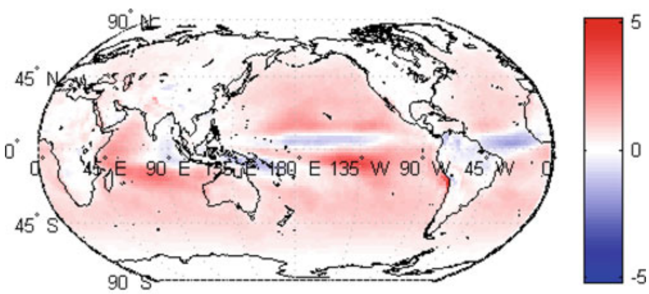

Fig. 6 Non-hydrostatic station height difference (ECMWF − NCEP); *colour bar* in mm

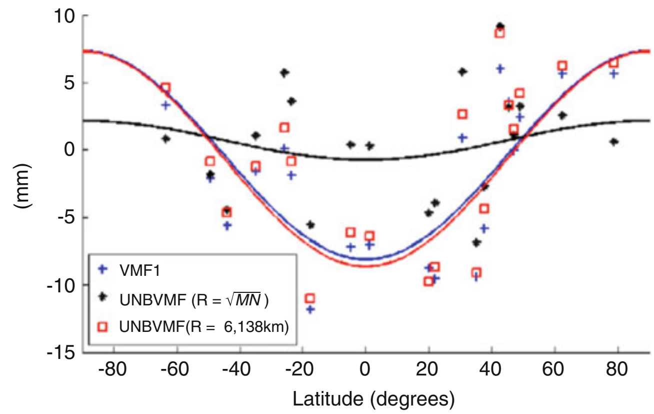

Fig. 7 Hydrostatic slant delay differences at the 5° elevation angle due to different radii of curvature. *Blue cross*: original VMF1, using a constant radius; *red squares*: UNB implementation using a constant radius; *black stars*: UNB implementation using the Gaussian radius. In this comparison, all UNB implementations used CMC-GEM data. The *lines* represent a least-squares fit of the data to the function a·cos(2ϕ) + c. Values in mm

4.3 Comparison of Mapping Functions

In these comparisons the following rule of thumb (Boehm et al. 2008) is used: "bias in station height is approximately equal to 1/5 bias in slant delay at 5° elevation angle."

The difference in station height due to mapping functions are shown in Fig. 5 (for the hydrostatic) and in Fig. 6 (for the non-hydrostatic). It shows a very small bias for both components: 0.8 ± 0.9 and 0.4 ± 0.6 mm, respectively. Notice that for the hydrostatic we see positive bias over the oceans and negative bias over land. Possible reasons for this, still in need of in-depth investigation, are: (a) the orography model used (currently we are using ECMWF orography); (b) partly due to differences in treatment of Earth's radius (see next paragraph).

The effect of Earth's radius on slant hydrostatic delay is discussed as follows. A local approximation to the ellipsoid can be represented by a normal sphere, i.e., whose radial direction coincides with the ellipsoid normal point on the surface. The radius of such a normal sphere can be computed in various ways. The most accurate is using Euler's formula:

$$R = \left(\frac{\cos^2 \alpha}{M} + \frac{\sin^2 \alpha}{N} \right), \tag{4}$$

where M is the radius of curvature of the meridian section and N is the radius of curvature of the prime vertical section, and α is the azimuth from the grid node to the satellite. Notice that this atmospheric structure of type Eulerian normal spherical does *not* yield azimuthally symmetrical delays. Another way of computing the spherical radius is the Gaussian radius of curvature:

$$R = \sqrt{MN} \tag{5}$$

Only in this case the normal sphere is said to be an osculating sphere. Notice that although the radius is azimuth-independent it is still latitude-dependent. Yet another way of computing the radius of the normal sphere is as a constant, for all latitudes and azimuths, as is the case of the VMF1. Finally, in the limit of infinite radius, we obtain a flat-Earth or tangent plane atmospheric structure (Nievinski and Santos 2010).

The choice of radius of curvature can indeed cause a bias. Figure 7 shows three solutions spanning over latitude, for the original VMF1 and two UNB implementations, one using a constant radius, similar to the VMF, and one using Eq. (5). In this case, all UNB solutions use the CMC-GEM analysis. As a reference solution, full three-dimensional ray-tracing through the CMC-GEM was used (see Nievinski 2009 for more details). The use of a constant radius causes a 15-mm peak-to-peak variation in the slant delay (approx equal to ±2 mm in station height) at the 5° elevation angle. Even with the Gaussian radius (black line) there is still a small latitude-dependent bias, but it is negligible in terms of error in station height.

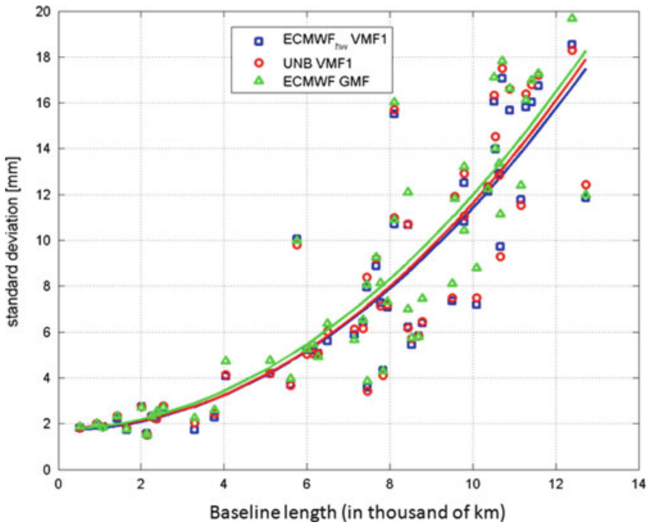

Fig. 8 Non-hydrostatic station height difference (ECMWF − NCEP). Values in mm

4.4 VLBI Results

Three solutions were used to process CONT08 (Teke et al. 2011) VLBI data sets: GMF (using a priori zenith delays derived from the ECMWF), VMF1 (using ECMWF), and UNB-VMF1 (using NCEP data). Gridded data was used. Results for baseline repeatability are shown in Fig. 8. Both VMF1's show improvement over the GMF, especially for longer baselines. The ECMWF VMF1 has the best performance overall. This may be due to the larger noise seen in the UNB a priori zenith delays. GMF repeatability worsens with baseline length; UNB-VMF1 follows VMF1 very well except for the very long baselines.

5 Concluding Remarks

Numerical weather models will continue to improve. As they do, they will become more useful for geodetic purposes. We have been generating VMF1-type grids using NCEP and GEM models at UNB. This is an attempt to satisfy consistency and redundancy issues.

Tests reported in this paper show that (a) zenith delays differences between VMF1 using ECMWF and NCEP are equal to -2.4 ± 3.8 mm for the hydrostatic, and -6.3 ± 14.7 mm for the non-hydrostatic components; (b) comparison to Saastamoinen showed a 2 mm (bias) and a 4 mm (st. dev.) and indicated that our use of NCEP was noisier than GEM; (c) difference in station height between ECMWF and NCEP showed a 0.8 ± 0.9 mm for the hydrostatic and -0.4 ± 0.6 mm for the non-hydrostatic components; (d) the impact of different radius of curvature was investigated, showing a latitude-dependent $\pm$ 2-mm height difference, largest at the poles and the equator; and finally, (e) impact on baseline repeatability using VLBI CONT08 data sets showed that the solutions using VMF1 and UNB-VMF1 are closer together than GMF, which got higher values.

As the UNB-VMF1 implementation gets developed in the future months, more tests are planned, including comparisons in the position domain using GPS campaigns and a look at effect on mean station position.

The future provision of UNB-VMF1 to the public will be similar to the current VMF1 service and will act as a backup or alternative for users.

Acknowledgments The authors acknowledge Matthias Madzak (TU Vienna) for processing the VLBI results, the weather agencies (ECMWF, NCEP and CMC) for providing access to the NWM data, and Natural Sciences and Engineering Research Council of Canada (NSERC) and the Austrian Science Fund (FWF, project P20902) for funding the research. Dow et al. 2009 is kindly acknowledged for the IGS products

References

Boehm J, van Dam T (2009) Modeling deficiencies and modeling based on external data. In: Second GGOS unified analysis workshop, IERS, Grand Hyatt, 11–12 December (oral presentation)

Boehm J, Niell AE, Tregoning P, Schuh H (2006a) Global Mapping Function (GMF): a new empirical mapping function based on numerical weather model data. Geophys Res Lett 33:L07304. doi:10.1029/2005GL025546

Boehm J, Werl B, Schuh H (2006b) Troposphere mapping functions for GPS and very long baseline interferometry from European Centre for medium-range weather forecasts operational analysis data. J Geophys Res 111:B02406. doi:10.1029/2005JB003629

Boehm J, Kouba J, Schuh H (2008) Forecast Vienna mapping functions 1 for realtime analysis of space geodetic observations. J Geodesy 83(5):397–401. doi:10.1007/s00190-008-0216-y

Dow JM, Neilan RE, Rizos C (2009) The international GNSS Service in a changing landscape of global navigation satellite systems. J Geodesy 83:191–198. doi:10.1007/s00190-008-0300-3

Fund F, Morel L, Mocquet A (2009) Discussion and recommendations about the height correction for a priori zenith hydrostatic delays derived from ECMWF data [on-line]. www.hg.tuwien.ac.at/~ecmwf1/Reducing_ECMWF_ZHDs.pdf

Herring TA (1992) Modelling atmospheric delays in the analysis of space geodetic data. In: de Munck JC, Th Spoelstra TA (eds) Proceedings of the symposium refraction of transatmospheric signals in Geodesy, No. 36, Netherlands Geodetic Commission, The Hague, 19–22 May, pp. 157–164

Kouba J (2008) Implementation and testing of the gridded Vienna Mapping Function 1 (VMF1). J Geodesy 82(4):193–205. doi:10.1007/s00190-007-0170-0

Marini JW (1972) Correction of satellite tracking data for an arbitrary tropospheric profile. Radio Sci 7(2):223–231. doi:10.1029/RS007i002p00223

Niell AE (1996) Global mapping functions for the atmosphere delay at radio wavelengths. J Geophys Res 101(B2):3227–3246. doi:10.1029/95JB03048

Nievinski FG (2009) Ray-tracing options to mitigate the neutral atmosphere delay in GPS. M.Sc.E. Thesis, Department of Geodesy and Geomatics Engineering technical report no. 262, University of New Brunswick, Fredericton, New Brunswick, 232 pp

Nievinski FG, Santos MC (2010) Ray-tracing options to mitigate the neutral atmosphere delay in GPS. Geomatica 64(2):191–207

Petit G, Luzum B (eds) (2010) IERS conventions (2010) (IERS technical note; 36). Verlag des Bundesamts für Kartographie und Geodäsie, Frankfurt am Main, 179 pp

Saastamoinen J (1972) Atmospheric correction for the troposphere and stratosphere in radio ranging of satellites. In: Henriksen SW, Mancini A, Chovitz BH (eds) The use of artificial satellites for Geodesy, vol. 15 of Geophysical monograph series. American Geophysical Union, Washington, DC, pp 247–251. ISBN 0-87590-015-1

Teke K, Böhm J, Nilsson T, Schuh H, Steigenberger P, Dach R, Heinkelmann R, Willis P, Haas R, García-Espada S, Hobiger T, Ichikawa R, Shimizu S (2011) Multi-technique comparison of troposphere zenith delays and gradients during CONT08. J Geodesy 85(7):395–413. doi:10.1007/s00190-010-0434-y

Tesmer V, Boehm J, Heinkelmann R, Schuh H (2007) Effect of different tropospheric mapping functions on the TRF, CRF and position time-series estimated from VLBI. J Geodesy 81:409–421. doi:10.1007/s00190-006-0126-9

Urquhart L (2010) Assessment of tropospheric slant factor models: comparison with three dimensional ray-tracing and impact of geodetic positioning. M.Sc.E thesis, Dept of Geodesy and geomatics Engineering technical report 275, University of New Brunswick, Fredericton, 166 pp